Petroleum Science 20 (2023) 3143–3156

Contents lists available at ScienceDirect

Petroleum Science

journal homepage: www.keaipublishing.com/en/journals/petroleum-science

Original Paper

Natural aging mechanism of buried polyethylene pipelines during long-term service

Ying-Chun Chen [a], Yan-Feng Li [a], Yan Xi [a,*], Qiang Li [b], Qi Lu [a], Jie Yang [a]

[a] Beijing University of Technology, Beijing, 100124, China
[b] Xinjiang Inspection Institute of Special Equipment, Urumqi, 830011, Xinjiang, China

ARTICLE INFO

Article history:
Received 4 December 2022
Received in revised form
1 March 2023
Accepted 1 March 2023
Available online 6 March 2023

Edited by Jia-Jia Fei

Keywords:
Polyethylene
Buried pipelines
Long-term service
Natural aging

ABSTRACT

Currently, accelerated aging tests are widely used to study the aging process of polyethylene pipelines. However, this approach can only simulate one or several main influencing factors in the natural environment, which are often quite different from the actual environment of the buried pipelines. In this study, five types of PE80 buried pipelines in service for 9–18 years were taken as the research object, while new PE80 pipelines were taken as the reference group. The aging process and mechanism of polyethylene buried pipelines were studied through mechanical and chemical property tests and microstructural analysis. The results showed that the pipeline exhibited cross-linking as the main aging mechanism after being in service for 0–18 years. The aging degree and law of the inner and outer surface of the pipeline were compared, and the observed mechanism of both surfaces was explained. After 18 years in service, the elongation at the break of the pipe decreased by 16.2%, and the toughness of the matrix in the main collapse area of the tensile sample was the fundamental reason responsible for changes in the mechanical properties. Finally, after 18 years in service, the oxidation induction time of the pipeline was 25.7 min, which was 28.5% higher than the national standard value. There were no potential safety hazards during continuous long-term service. The results of this paper provide reference data and theoretical guidance for the aging process study of buried polyethylene pipelines.

1. Introduction

Polyethylene pipelines are widely used in the oil and gas transportation industry because of their excellent machining performance, strong corrosion resistance, and low price (Taherinejad et al., 2017; He et al., 2018). However, polyethylene pipes also have some shortcomings (Contino et al., 2018; Khademi-Zahedi, 2019). The chemical structures of both medium and high-density polyethylene contain linear portions and double bonds. After long-term service, natural aging occurs that significantly reduces the performance and shortens the service life of the pipelines. Therefore, changes in the performance and service life of polyethylene pipelines during service have become the focus of several researchers (An et al., 2022; Wang Q. et al., 2021; Gholami et al., 2020).

At present, the research methods of polyethylene aging are mainly divided into natural aging and accelerated aging. Accelerated aging tests force a material to age quickly to obtain the aging degradation process and predict the service life of the pipeline. However, the disadvantage is that only a single or several main environmental factors can be simulated, which is quite different from the real pipeline service environment. According to the aging factors, accelerated aging tests can be divided into thermal-oxidative aging, hydrothermal aging, or ultraviolet aging (Hsueh et al., 2020; Fairbrother et al., 2019; Hedir et al., 2020). Researchers have conducted many experiments, and the research schemes and experimental results are relatively mature (Becerra and d'Almeida, 2017; Li et al., 2015; Bhowmick and White, 2002).

Weon (2010) studied the variation of thermal behavior and mechanical properties of low-density polyethylene pipelines with heat exposure time through thermal-oxidative aging experiments. The results showed that upon increasing the aging time, the hardness of the pipe increased slightly, and the elongation at break decreased. Wang Y. et al. (2021) conducted a photo-oxidative accelerated aging test on PE80 polyethylene pipes. A comprehensive pipeline performance evaluation method was established, and

* Corresponding author.
E-mail address: xiyan@bjut.edu.cn (Y. Xi).

https://doi.org/10.1016/j.petsci.2023.03.001

the aging process was divided into two stages. Therias et al. (2021) conducted UV accelerated aging experiments on low-density polyethylene films, and the results showed that the effects of light and temperature must be distinguished. There were differences in the mechanisms of thermal and photo-oxidative aging. The conclusion also indicates that accelerated aging has serious shortcomings when used to simulate the aging of in-service pipelines, as they can only reflect the influence of a single condition on polyethylene aging, which is quite different from the actual service situation. Chen et al. (2019) designed a new type of thermal oxidative accelerated aging test that involved applying different constant internal pressure cycles while changing the temperature. Compared with the ordinary thermal oxygen aging test, this method was more similar to the actual service conditions. However, the natural environment is more complex and changeable. Even the accelerated aging method coupled with temperature and pressure cannot simulate the service environment effectively.

Natural aging is the most effective and practical method for studying polyethylene pipeline aging (Lu et al., 2012; Ojeda et al., 2011). However, natural aging requires long times, and the pipe specifications are usually different. Therefore, it is difficult to study the natural aging trends of buried pipelines, and there are few reports in related fields. Natural aging can be divided into two categories. Some scholars have placed new polyethylene pipelines in a natural environment for aging tests. Gong et al. (2021) conducted a 24-month natural aging test on HDPE pipelines to study the effect of sunlight on the degradation of pipes. However, the service life of a pipeline can exceed 50 years, so the 24-month aging test cycle was too short to reflect the degradation mechanism of pipelines at different aging stages. Other scholars chose the serviced pipelines for testing, and obtained more reliable data. Kong et al. (2021) studied the performance and microstructure of polyethylene pipeline lining on the inner surface of steel pipes after 4 years in service. The results showed that polyethylene aged due to the expansion of the internal transmission medium. Both the mechanical and chemical properties decreased. Frank et al. (2009) and Bachir-Bey and Belhaneche-Bensemra (2020) studied the aging of polyethylene pipelines after 30 years in service. Due to aging conditions, the diameter and color of the pipeline were different, and the service time was irregular.

Therefore, using a buried pipeline as the research object has the highest practical value for engineering applications. The common characteristics of material properties with service time can be understood. However, the aging research on polyethylene pipelines has mainly focused on the artificially accelerated aging stage in the laboratory, which can only explain the aging process of polyethylene pipelines under the influence of a specific factor and do not reflect actual service conditions. Therefore, the obtained aging mechanism does not represent the aging mechanism of a service pipeline in a complex natural environment. In addition, obtaining an accurate and reliable conversion relationship between the artificially accelerated aging test and the natural serviced aging results is difficult. After many years of buried service, the performance status of the polyethylene pipeline remains still unknown. Therefore, many polyethylene service pipeline samples are needed as experimental data to systematically study the change law of pipe performance with service time and related mechanisms.

In this paper, five types of polyethylene buried pipelines in service for 9, 11, 13, 16, and 18 years were used as the research object, and new pipelines were used as the reference objects. The aging mechanism of buried pipelines was studied through mechanical and chemical property tests and microstructural analysis. The results provide data reference and theoretical guidance for the polyethylene aging study.

2. Experimental

2.1. Material

The experimental materials consisted of five different PE80 polyethylene buried pipelines according to their service years (9, 11, 13, 16, and 18 years) in China's natural gas buried pipeline network. The photos of buried pipelines are shown in Fig. 1. For comparison, PE80 polyethylene pipelines produced in 2021 were selected as the new group.

The parameters of the in-service pipelines are shown in Table 1, where DN is the nominal diameter of the pipe, and SDR is the standard size ratio. The test results in the experiment are obtained by taking the average value of multiple measurements.

2.2. Environmental parameters

The service area of the buried pipeline was the urban gas pipeline network in Tianshan District, Urumqi, China. Urumqi has a temperate continental climate with a large temperature difference between day and night. According to the data provided by the Urumqi Meteorological Station, the annual average temperature in the Tianshan District in the past three years was 7.3 °C. The highest temperature typically occurs in July, with an average temperature range of 25.4–26.2 °C. The lowest temperature is in January, when the average temperature is in the range of −14.3–15.2 °C. Moreover, the total annual solar radiation is about 513.98 kJ/cm^2, with about 2645 h of sunshine. The annual precipitation is about 248.9 mm.

Soil samples were taken from Tianshan District for analysis. The optimum moisture content of soil sample obtained from compaction test was 4.7%, and the maximum dry density was 2.3 g/cm^3. The soil organic matter (SOM) was about 47.7 g/kg, and the average pH was 7.8 (i.e., weakly alkaline soil). In addition, the soil in Urumqi is non-salinized soil, where the main salt is sulfate, and the total salt content is not more than 5 g/kg. The specific soil salt content is shown in Table 2.

According to the test data provided by Xinjiang inspection institute of special equipment, the natural gas components of buried pipeline are shown in Table 3.

2.3. Test method

2.3.1. Mechanical testing

Tensile properties were measured out on an ETM204C (WANCE, China) according to ISO 6259-1:2015 (2015). Fig. 2(a) shows the schematic diagram of the tensile sample size according to ISO 6259-3: 2015 (2015), and Fig. 2(b) shows the sample photograph. The tensile speed was 50 mm/min, and the strain was recorded with an extensometer. The test result was the average of five parallel samples.

Notch impact tests were performed on S8223X (SX, China) according to ISO 179-1: 2010 (2010). Before the test, the samples were machined with a notch with a 45° angle and a 2 mm depth. Fig. 3(a) shows a schematic of the notched impact sample size, and Fig. 3(b) shows a photograph of the sample. The energy of the test pendulum was 4 J, and the impact speed was 2.9 m/s. The reported test result was the average of five parallel samples.

The surface hardness of the pipeline sample was measured by LX-D (SUNDOO, China) according to ISO 868-2003 (2003). During the test, the sample was placed on a horizontal plane, and 10 points were selected on the same surface. The distance between each point was at least 6 mm. The reported test result was the average of 10 points.

Fig. 1. Photos of buried pipelines in service; (**a**) 9 years in service, (**b**) 13 years in service, and (**c**) 18 years in service.

Table 1
Parameters of buried pipelines.

Specimen	Material grade	DN, mm	SDR	Service time, year
1	PE80	63	11	0
2		63	11	9
3		63	11	11
4		63	11	13
5		63	11	16
6		63	11	18

Table 2
Soil salt content in Tianshan District, Urumqi.

	K^+	Ca^{2+}	Na^+	Mg^{2+}	$SO4^{2-}$	Cl^-	HCO_3^-
Ion content, $g\cdot kg^{-1}$	0.047	0.318	0.254	0.046	0.683	0.154	0.239

Table 3
Natural gas composition of the buried pipeline.

Components	Standard value, %	Measured value, %	Relative error, %
N_2	0.5370	0.5347	0.0023
CH_4	94.0830	94.0865	−0.0035
CO_2	1.5900	1.5796	0.0104
C_2H_6	2.8400	2.8386	0.0014
C_3H_8	0.5020	0.5007	0.0013
C_6H_{14}	0.0490	0.0473	0.0017

2.3.2. *Oxidation induction period*

The oxidation induction time (OIT) was measured with a DSC-500B (INNUO, China) according to ISO 11357–6: 2018 (2018). The sample was cut from the pipe surface, and the sample mass was 15 ± 0.5 mg. The crucible temperature rose from room temperature to 300 °C at a heating rate of 20 °C/min.

2.3.3. *Infrared spectra*

The chemical structure of the inner and outer surfaces of the samples was recorded by an FTIR-650S spectrometer (GANGDONG, China). The scanning frequency was 32, the resolution was 4 cm^{-1}, and the wavenumber range was 400–6000 cm^{-1}. The dust on the sample surface was cleaned before analysis.

2.3.4. *SEM*

The scanning electron microscopy (SEM) images of the pipeline surface were obtained by a Helios 5 CX DualBeam (FEI, USA). Before the test, the dust on the sample surface was removed, and the sample surface was sprayed with platinum.

3. Results and discussion

3.1. *Mechanical properties*

Fig. 4 shows the mechanical properties of pipes with different service times. Fig. 4(a) and (b) show the tensile strength and elongation at the break of the serviced pipelines. It can be seen from Fig. 4(a) that the tensile strength continued to increase from 0 to 18 years, with a total increment of 10.3%. According to Fig. 4(b), the elongation at the break of the pipeline decreased by 11.7% in 0–9 years and 4.5% in 9–18 years. It indicates that the elongation at the break of buried polyethylene pipelines decreased rapidly in 0–9 years, and the decline rate gradually slowed down in 9–18 years.

Fig. 4(c) shows the impact strength of the serviced pipeline. From 0 to 9 years, the impact strength decreased by 10.2%, and in 9–18 years, a reduction of 8.9%. It can be seen that the impact strength decreased significantly in the first 18 years. Moreover, the impact strength showed the same law as the elongation at break, in which the decline rate from 9 to 18 years was lower than from 0 to 9 years.

Fig. 4(d) shows that the average surface hardness of the non-service pipeline was 64.78 HD. After 9–18 years in service, the surface hardness of each pipeline was similar (67.28–68.34 HD). The surface hardness of the pipeline increased by at least 3.8% after 9–18 years in service compared with the new pipeline. However, there was little difference in surface hardness between service years, which were all within 1.58% of each other.

According to the mechanical properties above, with the increase

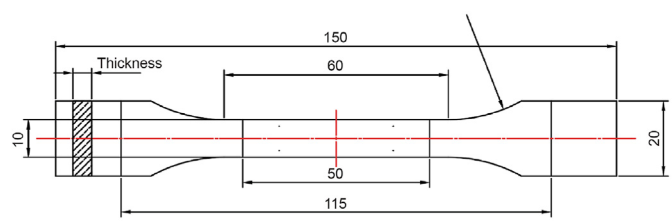

(a) Schematic of sample size

(b) Sample photograph

Fig. 2. Dumbbell tensile sample.

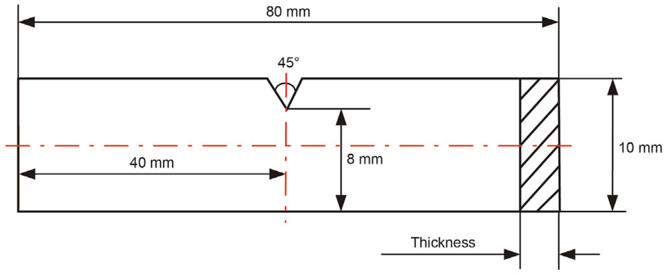

(a) Schematic of sample size

(b) Sample photograph

Fig. 3. Notch impact sample.

in service time, the tensile strength of buried pipelines continues to increase, and the elongation at break continues to decrease. It means that the pipe material gradually becomes hard and brittle during service, as noted by Hsueh and other scholars (Hsueh et al., 2020; Weon, 2010; Boubakri et al., 2011). Therefore, within 0–18 years in service, the degradation of polyethylene pipes occurred due to a cross-linking mechanism. However, in the later stage of aging, the surface layer peeled off in a large area, and cracks and pits appeared. This accelerated the aging process again, and chemical reactions easily occurred inside the material. During the oxidation reaction, carboxyl, ester, hydroxyl, and other functional groups were generated. Oxygen-containing functional groups promoted the large-scale fracture of –C=C– long chains, and the mechanical properties decreased. The crystallinity of the material was poor. Thus, it is predicted that the tensile strength will decline in the later stage of aging.

When polyethylene pipes are in service, there is almost no heat exposure to the environment, so its crystallite size and spherulite structure are difficult to change. However, O_2 in the soil oxidizes on the pipe surface and generates peroxide-type free radicals. These products trigger the cross-linking reaction of the long polyethylene chain as cross-linking agents. The generated cross-linking products are shown in Fig. 5.

3.2. Oxidation resistance

Oxidation induction time (OIT) refers to the time required to completely consume antioxidants in the sample and can reflect the consumption of antioxidants during the service life of buried pipelines.

It is generally believed that the antioxidants consumption rate in polyethylene pipelines follows the following exponential decay equation:

$$T(t) = T(0) \cdot e^{(-s \cdot t)} \tag{1}$$

where t is the service years of the pipeline, $T(t)$ is the OIT of the pipeline after t years' service, $T(0)$ is the OIT of the new pipeline,

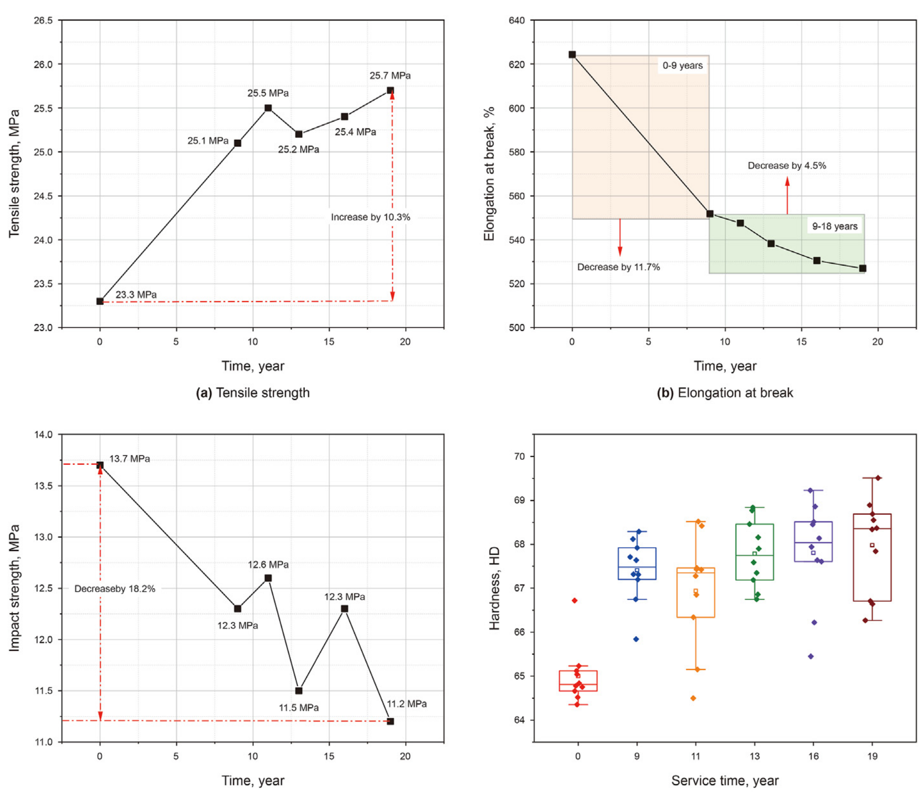

Fig. 4. Mechanical properties of pipelines with different service times.

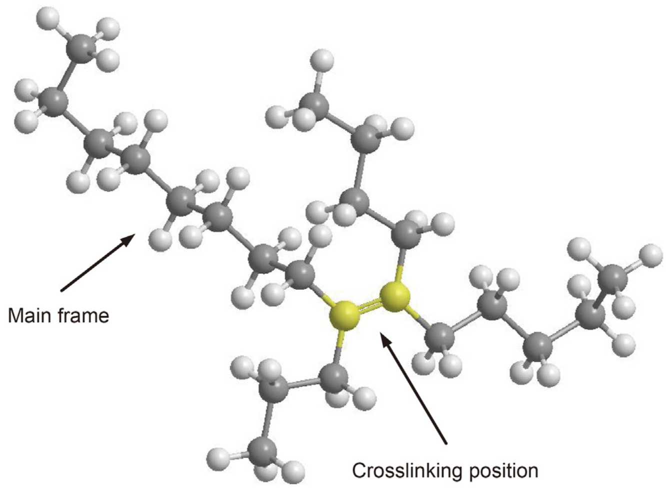

Fig. 5. Cross-linking mechanism of the polyethylene chain.

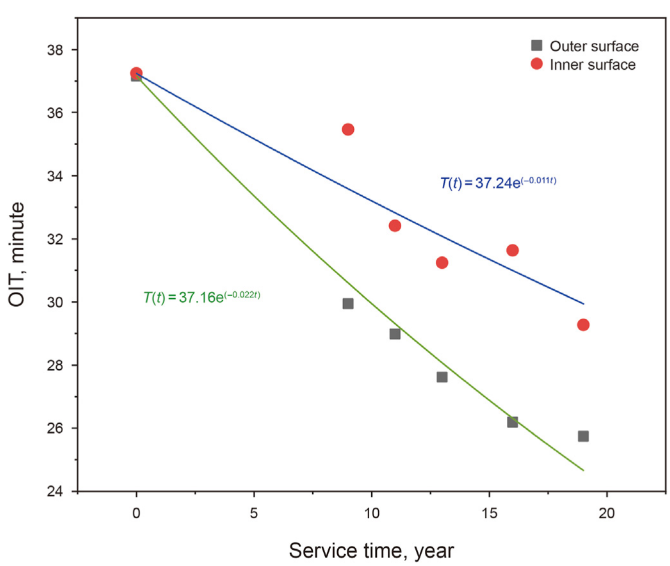

Fig. 6. OIT of polyethylene pipelines with different service times.

and s is the antioxidants consumption rate.

Fig. 6 shows the OIT of the inner and outer surfaces of the polyethylene pipelines with different service times. According to the OIT values, the attenuation equations of the antioxidant consumption rates of the inner and outer surfaces are fitted.

As shown in Fig. 6, the attenuation equation of the outer surface is as follows:

$$T(t) = 37.16e^{(-0.022t)} \quad (2)$$

The attenuation equation of the inner surface is as follows:

$$T(t) = 37.24e^{(-0.011t)} \quad (3)$$

According to Eqs. (2) and (3), the outer surface antioxidant consumption rate s_{out} is 0.022, and the inner surface antioxidant consumption rate s_{in} is 0.011. The antioxidant consumption rate on the outer surface is twice that of the inner surface. It is because the outer surface is in direct contact with the soil environment, and the oxides in the environment quickly consume the antioxidants on the outer surface. However, the inner surface is only in contact with transported oil and gas. The oxide content is low, and the antioxidant consumption rate is slower than that of the outer surface.

In addition, the minimum value of OIT specified in the national standard is greater than 20 min. In Fig. 6, the OIT value after 18 years in service is the lowest and is 25.7 min, which is greater than the value specified in the national standard. Therefore, after 18 years in service, polyethylene pipelines still have good oxidation resistance.

3.3. Infrared spectra

3.3.1. Comparison of inner and outer surfaces

Fig. 7 shows the infrared spectrum absorbance diagram of the inner and outer surfaces of polyethylene pipelines with the same service time. As shown in Fig. 7(a–c), each absorbance curve shows the methylene absorption peak of polyethylene at the four-wave positions of 2913, 2848, 1461, and 717 cm^{-1}. Besides, an absorption peak appears at 1143–948 cm^{-1}. It matches the stretching vibration of the oxidation functional group. It can be considered that there are alcohols, phenols, hydrocarbons, and other aging products on the pipeline surface after service. In addition, another absorption peak appears at 1695–1546 cm^{-1} after service. This matched the telescopic vibration of C=O and C=C. It shows that the pipeline surface has aging products of esters, carboxylic acids, aldehydes, and ketones.

After service, the absorption peaks of oxidation products on the outer surface are higher than those on the inner surface. It indicates that the aging of the pipeline begins at both the inner and outer surfaces. However, due to the direct contact between the outer surface and oxygen-containing substances in the soil environment, the aging of the outer surface is more severe than that of the inner surface with time.

In Fig. 7, the telescopic vibration peak on the outer surface of the pipeline was abnormally high at 1143–948 cm^{-1}. The infrared absorption peak of Si–O–Si is 1100–1000 cm^{-1}. Therefore, it is speculated that the outer surface is doped with SiO_2 (The outer surface of the sample was cleaned before the test). According to the energy spectrum shown in Fig. 8, the cleaned outer surface still contains high Si elements. Therefore, it is inferred that the absorption peak at 1024 cm^{-1} on the inner surface represents the oxidation functional group and that of the outer surface represents the common characterization of oxide functional groups and SiO_2.

3.3.2. Influence of aging time

Fig. 9 shows the infrared spectrum absorbance of the outer and inner surfaces of polyethylene pipelines with different service times. Compared with the new pipeline, the serviced pipeline has obvious absorption peaks at 1695–1546 and 1143–948 cm^{-1}. In addition, the serviced pipeline has small absorption peaks at 3550–3183 cm^{-1}.

Figs. 10 and 11 show the partially enlarged infrared absorbance spectra of the outer surface of polyethylene pipelines. Four absorption peaks appeared at 3550–3183, 1765–1705, 1695–1546, and 1143–948 cm^{-1} after service. Upon increasing the number of service years, the four absorption peaks enlarged. Both the absorption peaks at 3550–3183 and 1695–1546 cm^{-1} corresponded to –OH groups (Montes et al., 2012; Zha et al., 2023). There were two reasons for its generation: oxygen-containing substances and water contained within the materials. The absorption peak at 1143–948 cm^{-1} corresponded to the –C–O–C– group, which can be used to measure the aging degradation degree of the material with –OH groups. Additionally, the peak at 1695–1546 cm^{-1} corresponded to complex groups, including esters, ketones, aldehydes, and carboxylic acids. In Figs. 10(b) and Fig. 11(b), the organic products appeared after aging, and their content increased

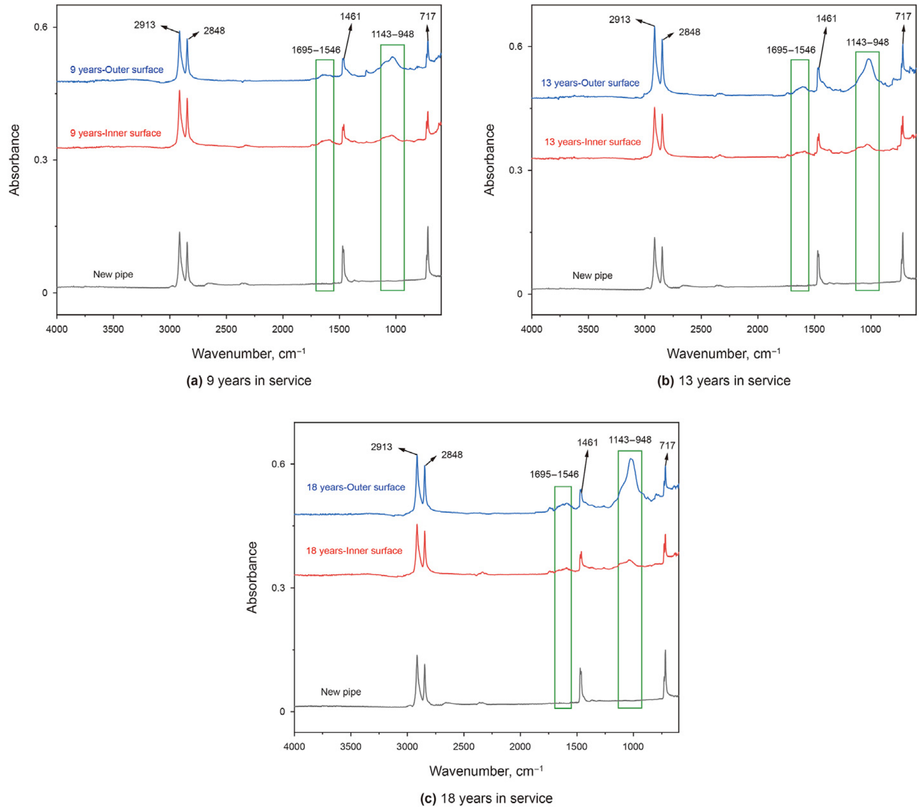

Fig. 7. Infrared spectral absorbance of inner and outer surfaces of polyethylene pipelines.

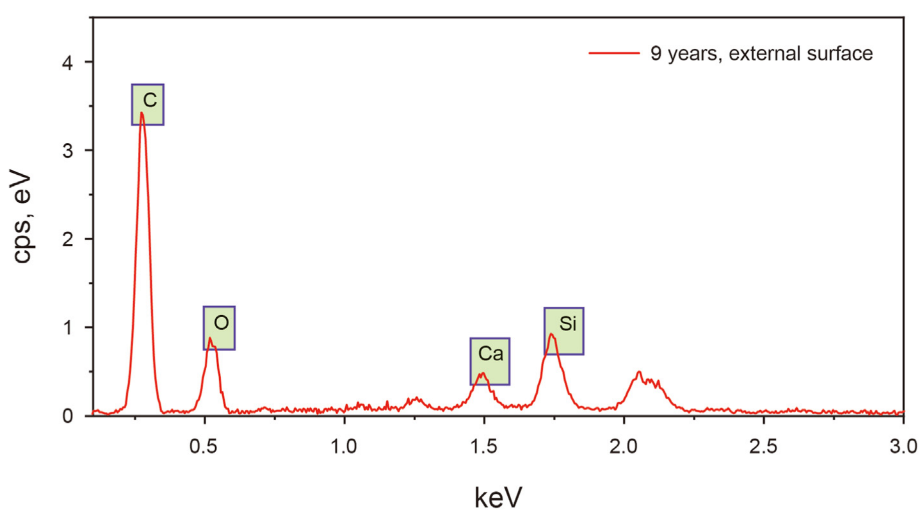

Fig. 8. Energy spectrum of the outer surface of 9 years serviced pipeline.

significantly.

3.4. Microstructural analysis

3.4.1. Microstructure of outer and inner surfaces

Fig. 12 shows the outer surface microstructure of polyethylene pipelines with different service times.

As shown in Fig. 12(a), due to processing and other factors, the outer surface of the new pipeline contains some scratches. Furthermore, there is no obvious aging on the surface. In Fig. 12(b), a large number of white particles appeared on the outer surface of the pipeline after 9 years in service, indicating that the outer surface of the pipeline began to age, and the surface degraded to produce debris. When aging begins, the molecular chain breaks and introduces carbonyl-dominated defective substances.

As shown in Fig. 12(c–f), as the service time increases, it can be seen that the potholes and roughness on the outer surface increase gradually. The aging degree is the most serious when the pipeline has been in service for 18 years. There are a lot of pits and impurities on the outer surface of the pipeline.

It also proves the aging process and mechanism of the pipeline: With the increase in service time, the antioxidants in the pipe are

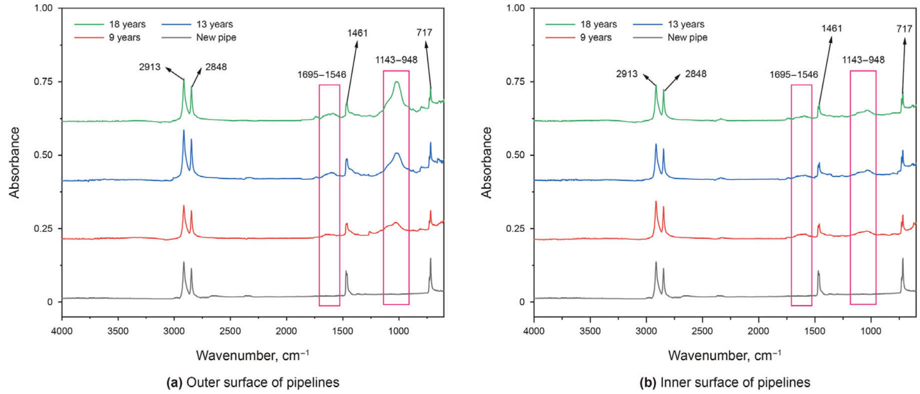

Fig. 9. Infrared spectrum absorbance diagram of polyethylene pipelines with different service time.

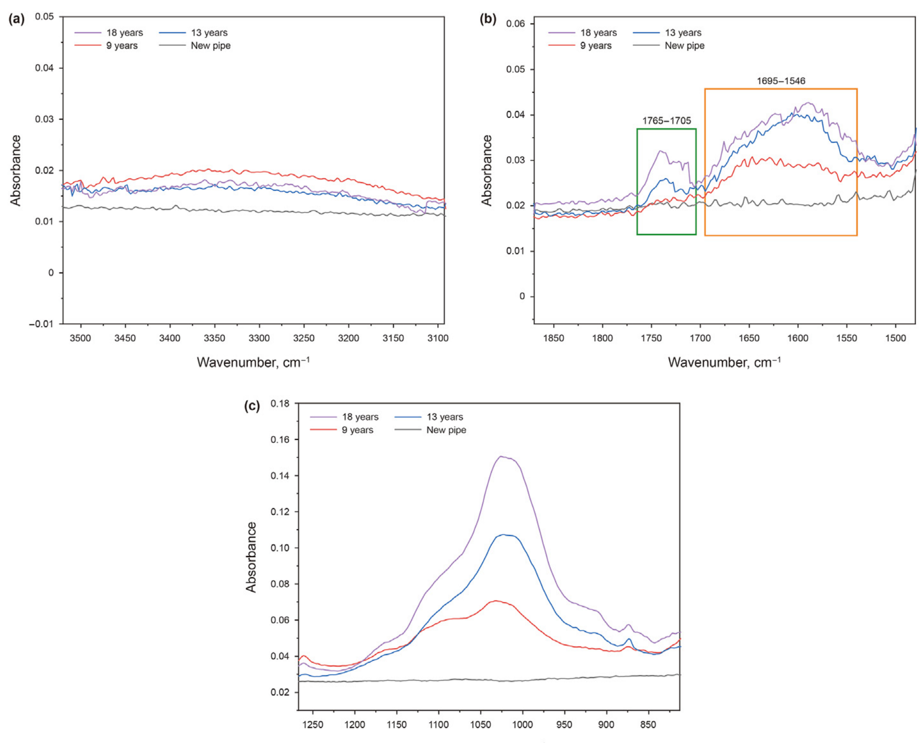

Fig. 10. Partially enlarged infrared absorbance spectra on the outer surface of polyethylene pipelines; (**a**) 3550–3183 cm^{-1}; (**b**) 1695–1546 cm^{-1}; (**c**) 1143–948 cm^{-1}.

gradually consumed, and the matrix begins to age. Water and oxygen in the soil environment lead to an oxidation reaction on the outer surface of the pipe. Macromolecular chains and short branched chains are broken to varying degrees. On the microstructure, white particles and impurities appear on the surface of the pipeline. As aging intensifies, they peel off and form pits. The longer the service time is, the more and deeper the pits are.

In addition, there is another explanation for the mechanism of the pits. Some scholars believe that the pits on the surface are related to the deterioration of surface mechanical strength and the competitive effect of anisotropic internal stress. The aging of the pipeline leads to the gradual decline of mechanical properties. When the mechanical strength cannot bear the internal stress, cracks appear. When the aging is severe, the cracks induce pits.

Fig. 13 shows the inner surface microstructure of polyethylene pipelines with different service times. After 9 years in service (Fig. 13(b)), white particles appeared on the inner surface. After 11 and 13 years in service (Fig. 13(c) and (d)), there were many small pits and lines on the surface. However, compared with the new pipeline (Fig. 13(a)), their inner surfaces are smoother without obvious scratches. When the service time reached 13 and 16 years (Fig. 13(e) and (f)), the depth of the pits on the inner surface deepened, and the range enlarged. The overall roughness of the inner surfaces increased, especially the pipeline in service for 16 years, whose pits connected and formed fine cracks.

Comparing Figs. 12 and 13, there is no obvious difference between the microstructure of the outer and inner surfaces of the new pipeline. However, the microstructure gradually varies with the service time when the pipeline is in service. Many irregular defects appear on the outer surface, and the aging degree is severe. In contrast, the inner surface is slightly aged, and only shallow pits are produced. It shows that the aging rate greatly relates to the exposed environment. The outer surface of the pipe is in direct contact with the soil. A large amount of H_2O and O_2 in the soil environment

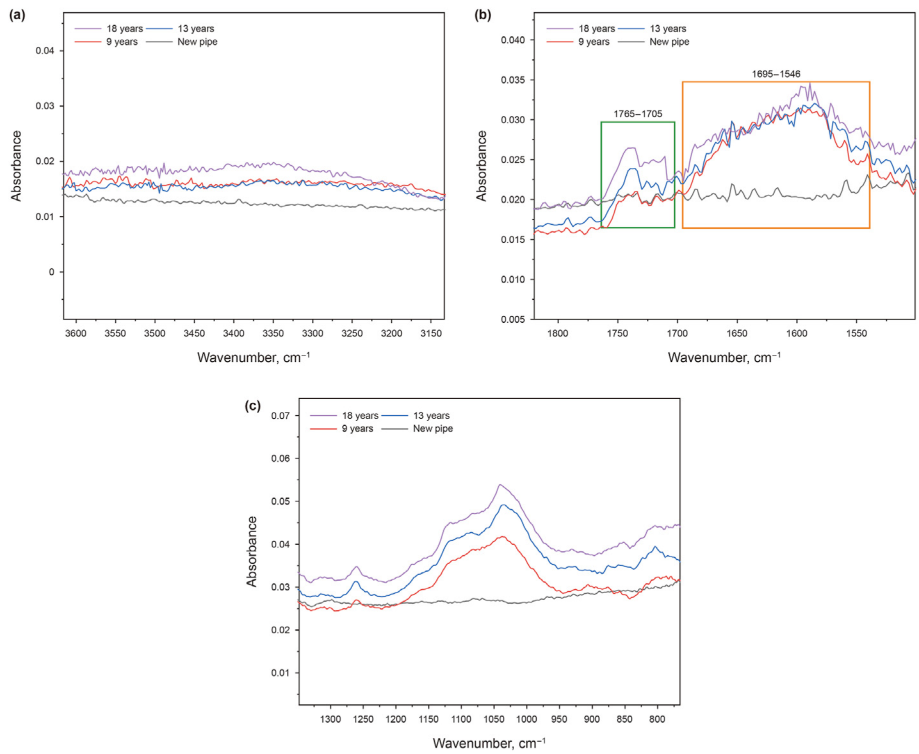

Fig. 11. Partially enlarged infrared absorbance spectra on the inner surface of polyethylene pipelines; (**a**) 3550–3183 cm^{-1}; (**b**) 1695–1546 cm^{-1}; (**c**) 1143–948 cm^{-1}.

accelerates the aging process. The inner surface is in contact with natural gas, which contains few oxidizing substances. Thus, the antioxidant consumption rate is slow, and the aging degree of the inner surface is relatively slight.

3.4.2. Microstructure of tensile fracture surface

According to the tensile test results in Section 3.1, the mechanical properties decrease significantly with the increase in service time. Both the tensile strength and elongation at the break of the tensile sample decreased. To explore the mechanism of pipeline aging on its mechanical properties, the microstructure of the fracture surface was observed by SEM. Fig. 14 shows the sample photos after the tensile test. It is seen in Fig. 14(b) and (c) that the fracture surface of the extended sample part is concave, and the fracture surface of the short sample part is a protruding surface.

The fracture surfaces of the long tensile fracture samples with a service time of 9, 13, and 18 years were selected for SEM. The microstructure of the fracture surfaces is shown in Fig. 15(a), Fig. 16(a), and Fig. 17(a).

Fig. 15 shows the microstructure of the tensile fracture surface that was in service for 9 years. As shown in Fig. 15(a), the yellow and blue lines represent division lines 1 and 2, respectively. The surface morphology of the fracture can be divided into three areas according to the division line: The main collapse area is inside division line 1. The buffer area is between division lines 1 and 2. The first fracture area is outside division line 2.

Fig. 15(b) and (c) show the microstructure near division lines 1 and 2, respectively. According to Fig. 15(b), the texture of the main collapse area (inside division line 1) is longitudinal stripes. The texture of the buffer area is a transverse stripe. Close to division line 1, the texture of the main collapse area gradually becomes a transverse stripe. Compared with it, the cracks near division line 2 and the first fracture area are deeper in Fig. 15(c).

In addition, the microstructure of three typical regions in Fig. 15(a) are identified as follows: the central hole of the fracture surface is shown in Fig. 15(d), and the side wall of the main collapse area is shown in Fig. 15(e), and the buffer area is shown in Fig. 15(f). It is seen in Fig. 15(e) and (f) that the fiber texture of the side wall of the main collapse area and the buffer area are significantly different. The section of the main collapse area shows fiber pullout, and the adhesion between the fiber and the surface matrix is less. Since the medium-density polyethylene is mainly in C=C configuration and has good ductility, it produces obvious filaments during elongation. The buffer area belongs to the outer layer of the elongation sample. In the elongation process, the sudden stress change in a short time is significant. Therefore, it breaks first, and the section does not produce obvious filaments.

Figs. 16 and 17 show the microstructure of the tensile fracture surfaces with 13 and 18 years in service, respectively. Comparing Figs. 15–17, it can be seen that there is no significant difference in the surface morphology of the central holes (Figs. 15(d), Fig. 16(b), Fig. 17(b)) and the first fracture area (Figs. 15(f), Fig. 16(d), Fig. 17(d)). However, through the surface morphology of the buffer area (Figs. 15(e) and Fig. 16(c), Fig. 17(c)), it is seen that with the increase in service time, the pullout of the fiber from the matrix gradually weakens, and the fiber filament is shorter. It indicates that with the increase in service time, the aging of the pipeline becomes severe, the C=C bond breaks, and the material ductility is weakened.

3.5. Ageing mechanisms of the pipelines

3.5.1. Aging periods of polyethylene buried pipeline

Fig. 18 shows the schematic diagram of the buried pipeline's aging process. Fig. 18(a) shows the sectional diagram of buried pipelines. The outer surface is in contact with the soil environment, and the inner surface is in contact with the transported natural gas.

According to the experimental results, the aging process of

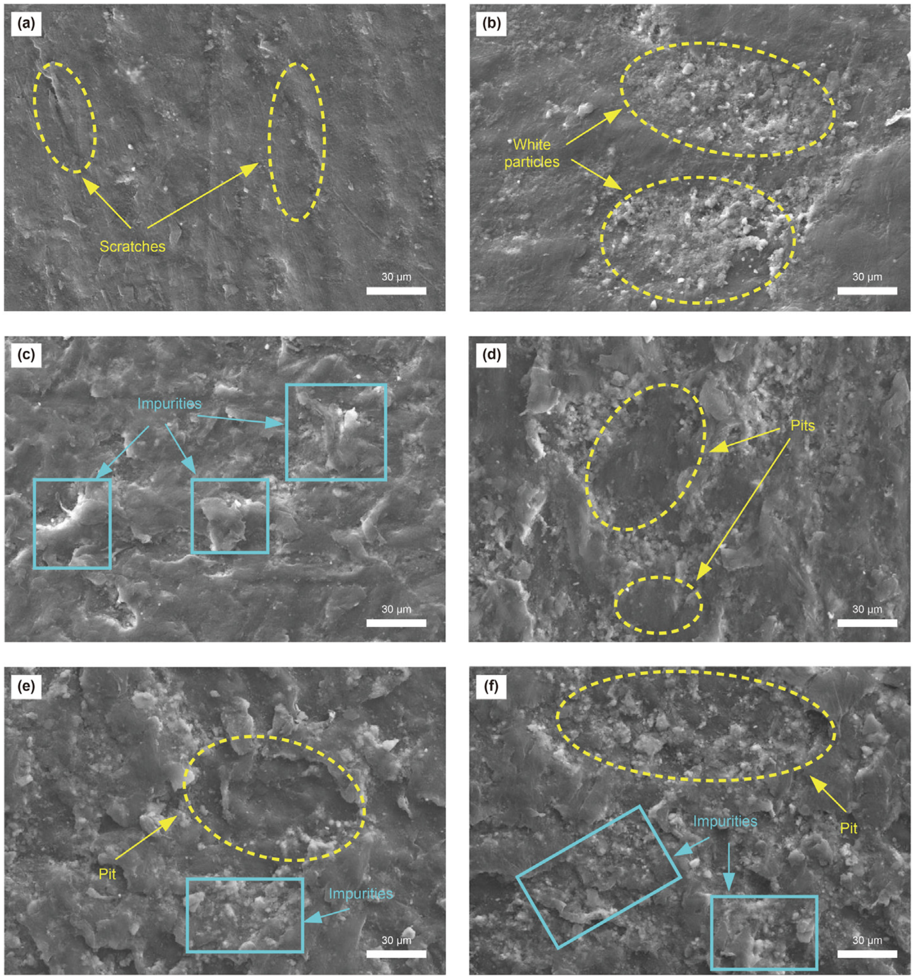

Fig. 12. The outer surface morphology of polyethylene pipelines with different service times: (**a**) New pipeline, (**b**) 9 years, (**c**) 11 years, (**d**) 13 years, (**e**) 16 years, and (**f**) 18 years.

buried service pipelines from 0 to 18 years can be divided into three periods: the early aging period, the slow aging period, and the significant aging period.

As shown in Fig. 18(b), the pipeline is in the early aging period within 0–9 years in service. Most buried pipelines contain anti-aging additives, which are mainly composed of antioxidants. Because the soil contains a lot of water molecules and oxygen, the antioxidants in the surface layer are consumed first in the early aging period. During the consumption of the surface antioxidants, the oxygen-containing elements in the soil start to react with the pipeline matrix. The C═C bond in polyethylene breaks and generates oxide. Therefore, the infrared spectrum shows the absorption peak corresponding to the oxidation product. Besides, white particles appear on the outer surface in Fig. 12(a) and (b).

It is seen in Fig. 18(c) that the pipeline is in the slow aging period within 9–13 years in service. An oxide layer formed on the pipeline's outer surface due to the accumulation of oxide products. It has a certain isolation effect on oxides in the external environment, which slows down the consumption rate of the antioxidants and the pipe matrix. Similarly, there is an aging product layer on the inner surface.

As shown in Fig. 18(d), the pipeline was in the significant aging period within 13–18 years in service. After long-term service, the oxide layer on the surface gradually becomes loose and falls off. Large areas of potholes and depressions appear on the outer surface, as shown in Fig. 12(e) and (f). The detached oxide layer made the oxide in the environment easier to react with the internal matrix. In the cycle, the pipeline's performance decreased significantly.

3.5.2. *Organic effects during aging*

Crystallinity changes and molecular chain cross-linking are important factors affecting mechanical properties. The chain breakage of entangled and cross-linked chain molecules in HDPE caused them to reorganize into a crystalline phase. Thus, the crystallinity increased (Hsueh et al., 2020; Fayolle et al., 2008) and the amorphous part in the matrix was removed. This caused embrittlement, as shown in the mechanical properties in Section 3.1. In addition, Colom (Colom et al., 2003) proposed that unsaturated bonds gradually formed and participated in branching and cross-linking reactions during aging. Compared with artificial accelerated aging, natural aging is more prone to cross-linking reactions.

Buried pipelines are exposed to less O_2 and H_2O in the soil environment. Additionally, the oxide film formed on the pipe surface prevents further aging. Therefore, the aging process of buried pipelines is much slower than that during artificial accelerated aging. Molecular configuration and chain entanglement are the main factors during the early stage of aging. Due to the −C═C− chain structure, molecular chain fracture, chain entanglement density, and chain mobility affect the material properties during aging. However, during the later stage of aging, many carboxyl,

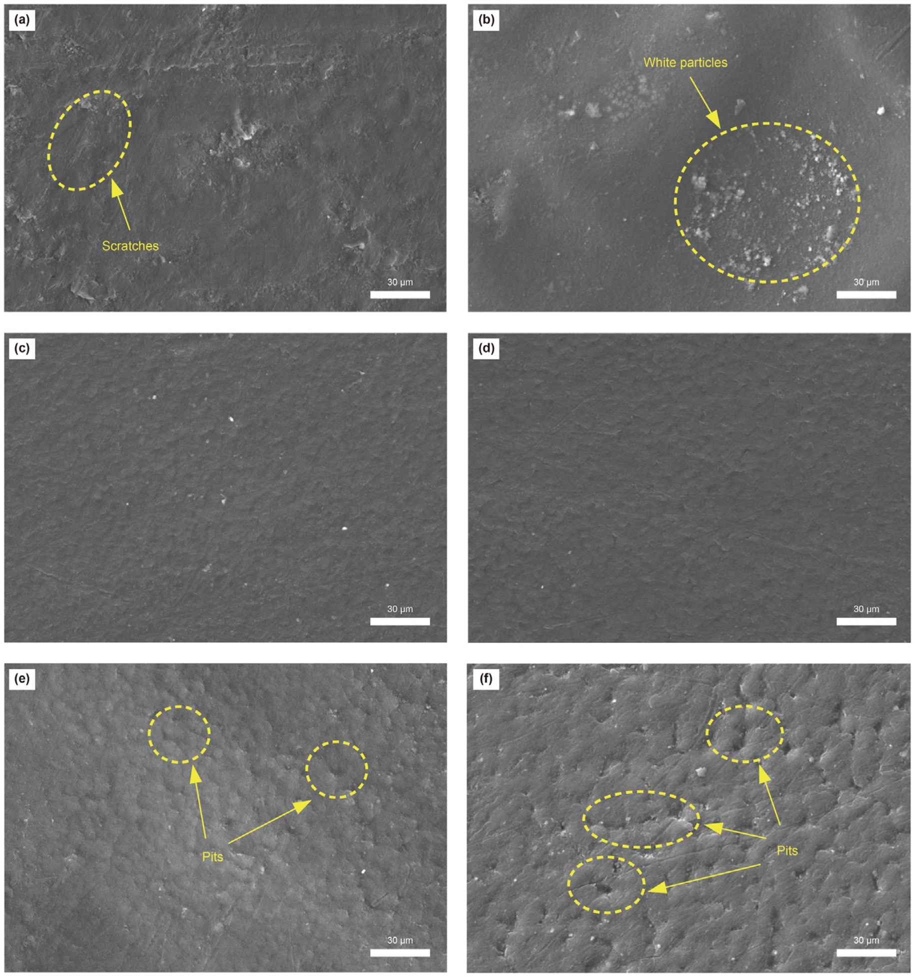

Fig. 13. The inner surface microstructure of polyethylene pipelines with different service times: (**a**) New pipeline, (**b**) 9 years, (**c**) 11 years, (**d**) 13 years, (**e**) 16 years, and (**f**) 18 years.

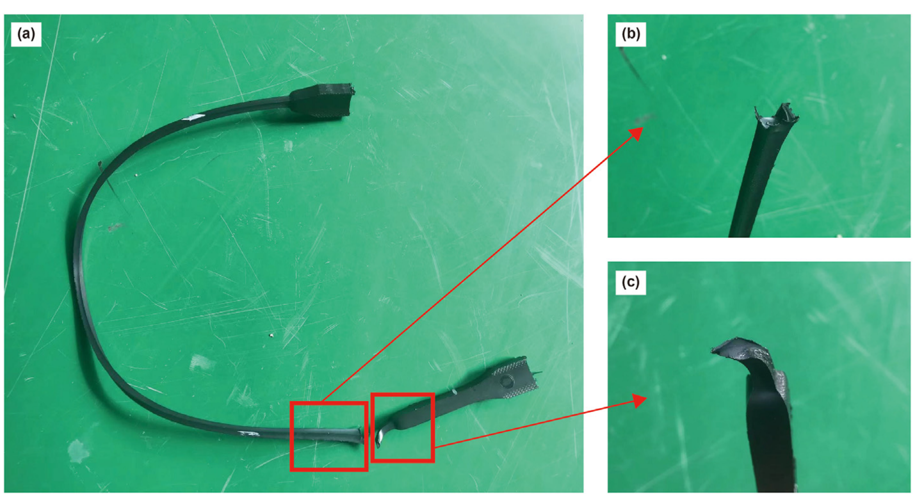

Fig. 14. Tensile fracture surfaces of polyethylene pipeline sample; (**a**) Fractured sample profile, (**b**) fracture surface of the extended sample part, and (**c**) fracture surface of the short sample part.

hydroxyl, ester, and other functional groups are formed due to oxidation of the HDPE molecular chain. Oxygen-containing functional groups promote large-scale chain breaking of −C=C− chains. At this time, chain scission is the dominant mechanism.

3.5.3. Aging difference between inner and outer surfaces

The aging mechanism of the inner and outer surfaces of polyethylene pipelines after long-term service is shown in Fig. 19. The service condition is shown in Fig. 19(a). The polyethylene pipeline is

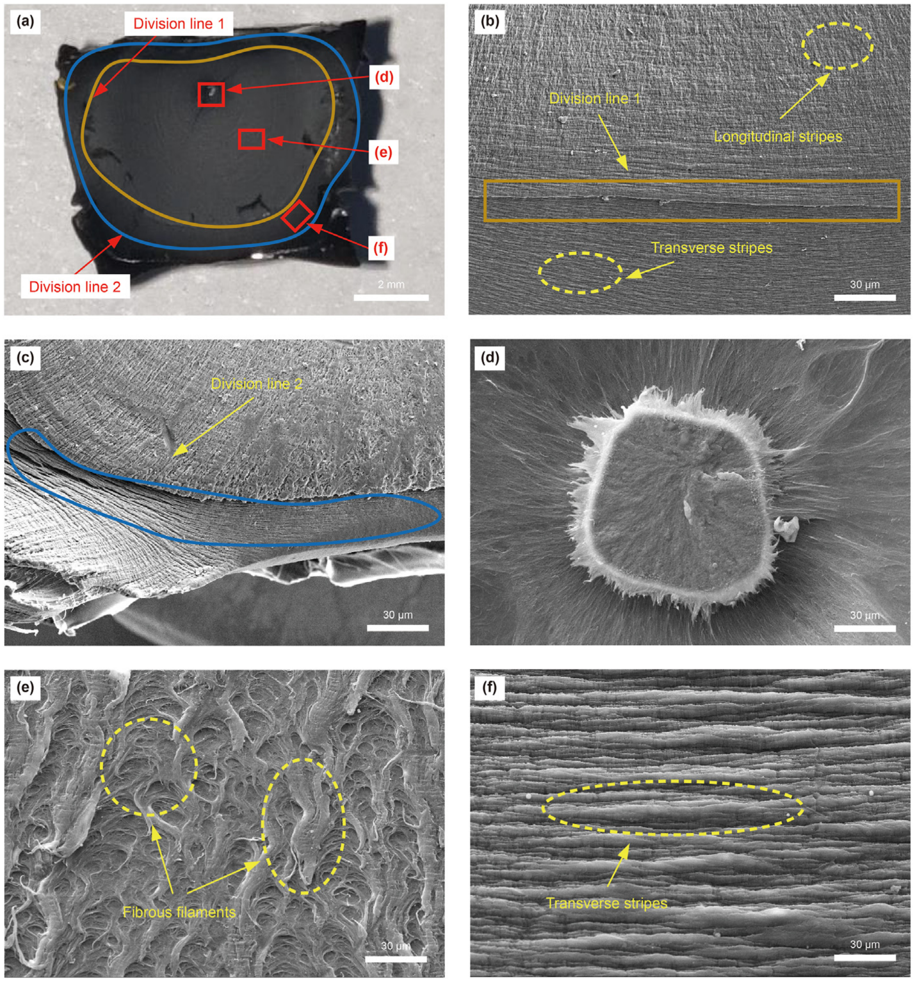

Fig. 15. Fracture surface of the tensile sample with 9 years' service; (**a**) Fracture surface image, (**b**) microstructure near division line 1, (**c**) microstructure near division line 2, (**d**) central hole, (**e**) main collapse area, and (**f**) buffer area.

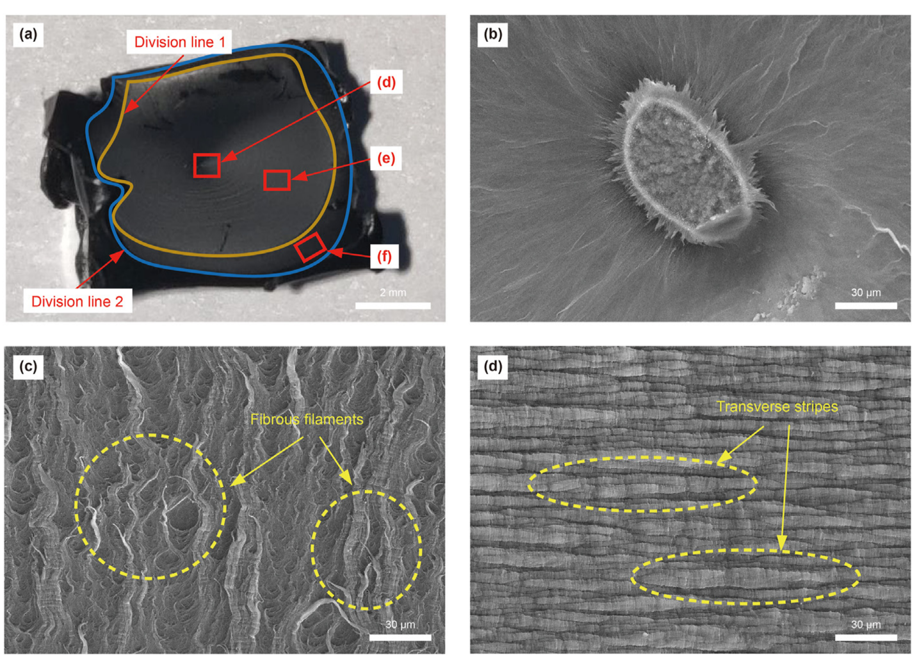

Fig. 16. Fracture surface of the tensile sample with 13 years' service; (**a**) Fracture surface image, (**b**) central hole, (**c**) main collapse area, and (**d**) buffer area.

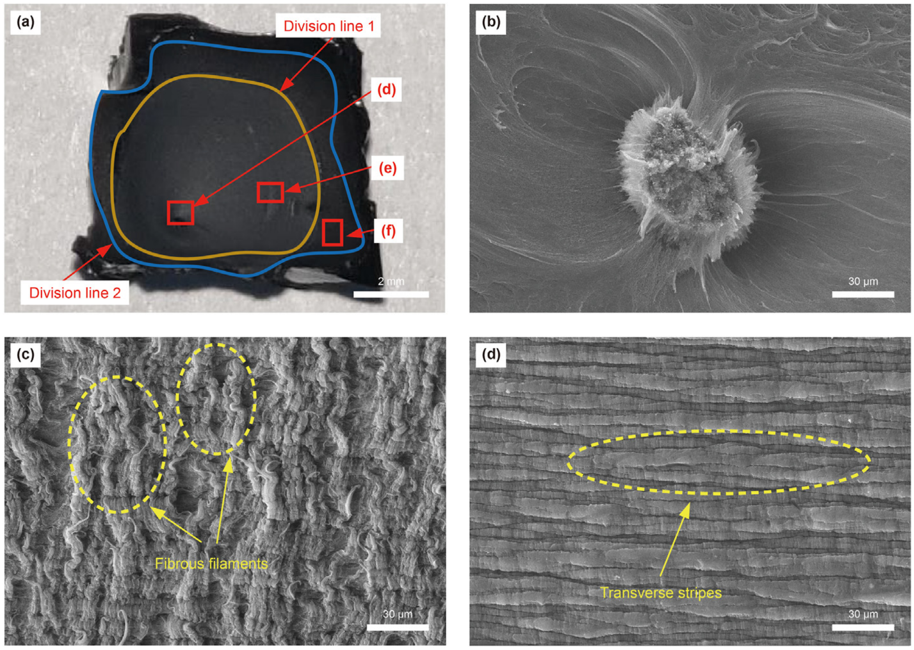

Fig. 17. Fracture surface of the tensile sample with 18 years' service; (**a**) Fracture surface image, (**b**) central hole, (**c**) main collapse area, and (**d**) buffer area.

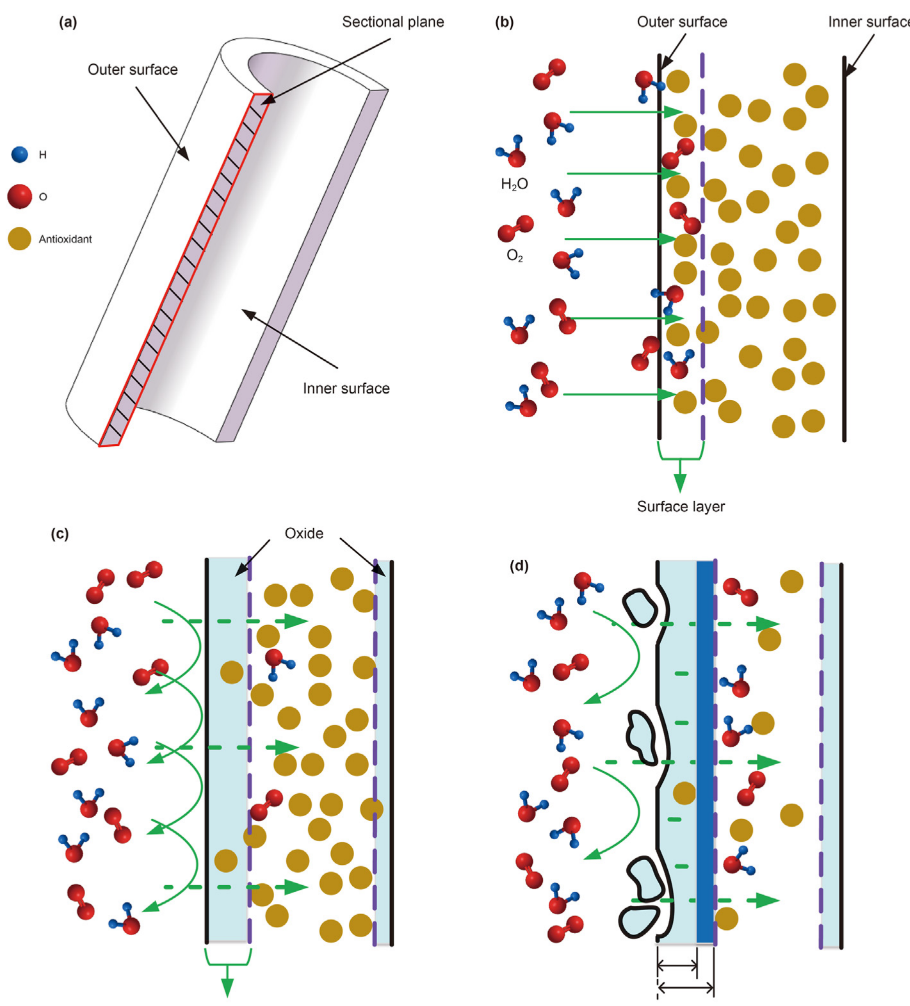

Fig. 18. Schematic diagram of buried pipelines aging process; (**a**) sectional diagram of the pipeline, (**b**) early aging period, (**c**) slow aging period, and (**d**) significant aging period.

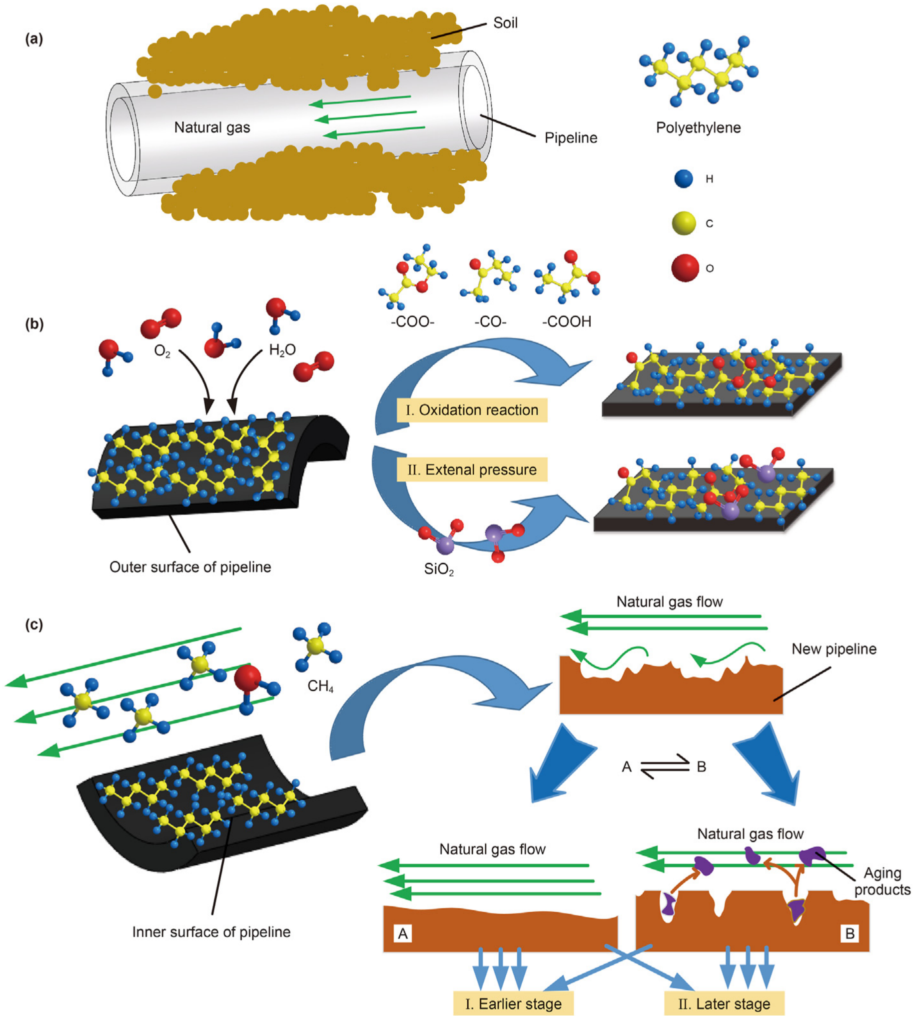

Fig. 19. Aging mechanism of the outer and inner surfaces of the polyethylene pipelines; (**a**) Service environment, (**b**) outer surface and (**c**) inner surface of the pipeline.

surrounded by soil, and the transportation pressure of the natural gas inside the pipeline can reach 0.4–0.7 MPa. The aging mechanism of the outer and inner surfaces is shown in Fig. 19(b) and (c), respectively.

As shown in Fig. 19(b), the outer surface of the pipeline is in direct contact with the environment. Because the soil contains a lot of water and oxygen, the outer surface is prone to oxidation reactions that age the pipeline. Oxidation generates carbonyl, carboxyl, aldehyde, and ester groups, but carbonyl production is the main aging factor. Besides, under long-term external pressure, SiO_2 is embedded in the outer surface of the pipeline. Therefore, Silicon atoms were detected in the infrared spectrum and energy spectrum.

Fig. 19(c) shows the aging mechanism of the inner surface of the pipeline. The main component of natural gas transported by pipeline is CH_4 which accounts for 94%. Natural gas contains only a small amount of oxygen-containing substances such as H_2O and CO_2, so it is difficult to have an oxidation reaction with the inner surface. Thus, the aging conditions of the inner and outer surfaces are quite different. The outer surface has obvious aging since 9 years, and the aging is severe at 16 and 18 years. However, obvious aging of the inner surface occurs only at 16 and 18 years.

In addition, the inner surface of the pipeline in Fig. 13 gradually exhibits roughness, flatness, and potholes with the service time. The formation was explained by the aging mechanism in Fig. 19(c). As shown in Fig. 13(a), scratches formed on the inner surface due to processing factors. The rough particles of the matrix increased the drag force on the inner surface during natural gas flows. Under the long-term circulation of natural gas inside the pipeline, the fluid polished the inner surface of the pipeline. Therefore, in Fig. 13(b–d), the inner surface was gradually flattened. After 16 and 18 years in service, antioxidant consumption and internal surface aging products increased gradually. Under the long-term flow of gas pipeline transportation, loose aging products are removed. When the air flows through the holes on the inner surface, the increased shear forces produce high-energy and small-scale turbulence that further expands the holes.

4. Conclusion

The mechanical properties of the pipeline decreased rapidly within 0–9 years and slowly within 9–18 years. The material crystallinity increased, and the branching and cross-linking reaction of the molecular chains dominated. Macroscopically, this produced a hard and brittle material. Due to the different environments between the inner and outer surfaces, after 9–18 years in service, the aging degree of the outer surface was much greater than that of the inner surface. The inner surface was pitted with different roughness values within 9–18 years, which was related to the hydrodynamic effect of the internal transportation gas on the pipe surface. Additionally, the tensile fracture surface was divided into three regions. Pipeline aging mainly changed the mechanical properties by affecting the matrix toughness in the main collapse area.

In terms of pipeline safety, after 18 years in service, the material properties were still far higher than those of the national standard. Therefore, the performance of the pipeline remained stable and normal, and it could continue long-term service without potential safety hazards. Reports on the natural aging behaviors of buried pipelines are few. Continuing to explore the aging laws in service pipelines under various typical landforms and soil environments can help establish a complete environmental load spectrum.

Declaration of competing interest

The authors declare that they have no known competing financial interests or personal relationships that could have appeared to influence the work reported in this paper.

Acknowledgments

Special technical support program of the State Administration of Market Supervision (2021YJ021), and Science and technology program of the State Administration of Market Supervision (2021MK118, 2021MK119).

References

An, Z., Tang, Q., Huang, Y., et al., 2022. Time-dependent analysis of buried high-density polyethylene (PE100) pipelines with a scratch defect subjected to touchdown impact loading of blasting collapsed body. Int. J. Pres. Ves. Pip. 195, 104605. https://doi.org/10.1016/j.ijpvp.2021.104605.

Bachir-Bey, T., Belhaneche-Bensemra, N., 2020. Investigation of polyethylene pipeline behavior after 30 Years of use in gas distribution network. J. Mater. Eng. Perform. 29, 6652–6660. https://doi.org/10.1007/s11665-020-05118-9.

Becerra, A.F.C., d'Almeida, J.R.M., 2017. UV effects on the tensile and creep behaviour of HDPE. Polym. Polym. Compos. 25 (5), 327–332. https://doi.org/10.1177/096739111702500502.

Bhowmick, A.K., White, J.R., 2002. Thermal, UV- and sunlight ageing of thermoplastic elastomeric natural rubber-polyethylene blends. J. Mater. Sci. 37 (23), 5141–5151. https://doi.org/10.1023/A:1021076724403.

Boubakri, A., Haddar, N., Elleuch, K., et al., 2011. Influence of thermal aging on tensile and creep behavior of thermoplastic polyurethane. CR. Mecanique. 339 (10), 666–673. https://doi.org/10.1016/j.crme.2011.07.003.

Chen, G., Yang, Y., Zhou, C., et al., 2019. Thermal-oxidative aging performance and life prediction of polyethylene pipe under cyclic and constant internal pressure. J. Appl. Polym. Sci. 136 (28), 47766. https://doi.org/10.1002/app.47766.

Colom, X., Canavate, J., Sunol, J.J., et al., 2003. Natural and artificial aging of polypropylene-polyethylene copolymers. J. Appl. Polym. Sci. 87 (10), 1685–1692. https://doi.org/10.1002/app.11613.

Contino, M., Andena, L., Rink, M., et al., 2018. Time-temperature equivalence in environmental stress cracking of high-density polyethylene. Eng. Fract. Mech. 203, 32–43. https://doi.org/10.1016/j.engfracmech.2018.04.034.

Fairbrother, A., Hsueh, H.C., Kim, J.H., et al., 2019. Temperature and light intensity effects on photodegradation of high-density polyethylene. Polym. Degrad. Stabil. 165, 153–160. https://doi.org/10.1016/j.polymdegradstab.2019.05.002.

Fayolle, B., Richaud, E., Colin, X., et al., 2008. Rewiew: degradation-induced embrittlement in semi-crystalline polymers having their amorphous phase in rubbery state. J. Mater. Sci. 43 (22), 6999–7012. https://doi.org/10.1007/s10853-008-3005-3.

Frank, A., Pinter, G., Lang, R.W., 2009. Prediction of the remaining lifetime of polyethylene pipes after up to 30 years in use. Polym. Test. 28 (7), 737–745. https://doi.org/10.1016/j.polymertesting.2009.06.004.

Gholami, F., Pircheraghi, G., Sarafpour, A., 2020. Long-term mechanical performance of polyethylene pipe materials in presence of carbon black masterbatch with different carriers. Polym. Test. 91, 106857. https://doi.org/10.1016/j.polymertesting.2020.106857.

Gong, Y., Wang, S.H., Zhang, Z.Y., et al., 2021. Degradation of sunlight exposure on the high-density polyethylene (HDPE) pipes for transportation of natural gases. Polym. Degrad. Stabil. 194, 109752. https://doi.org/10.1016/j.polymdegradstab.2021.109752.

He, X., Zha, X., Zhu, X., et al., 2018. Effect of short chain branches distribution on fracture behavior of polyethylene pipe resins. Polym. Test. 68, 219–228. https://doi.org/10.1016/j.polymertesting.2018.04.017.

Hedir, A., Moudoud, M., Lamrous, O., et al., 2020. Ultraviolet radiation aging impact on physicochemical properties of crosslinked polyethylene cable insulation. J. Appl. Polym. Sci. 137 (16), 48575. https://doi.org/10.1002/app.48575.

Hsueh, H.C., Kim, J.H., Orski, S., et al., 2020. Micro and macroscopic mechanical behaviors of high-density polyethylene under UV irradiation and temperature. Polym. Degrad. Stabil. 174, 109098. https://doi.org/10.1016/j.polymdegradstab.2020.109098.

ISO 11357-6: 2018, 2018. Plastics - Differential Scanning Calorimetry (DSC)-Part 6: Determination of Oxidation Induction Time (Isothermal OIT) and Oxidation Induction Temperature (Dynamic OIT). International Organization for Standardization, Geneva, Switzerland.

ISO 179-1: 2010, 2010. Plastics - Determination of Charpy Impact Properties - Part 1: Non-instrumented Impact Test. International Organization for Standardization, Geneva, Switzerland.

ISO 6259-1: 2015, 2015. Thermoplastics Pipes - Determination of Tensile Properties - Part 1: General Test Method. International Organization for Standardization, Geneva, Switzerland.

ISO 6259-3: 2015, 2015. Thermoplastics Pipes - Determination of Tensile Properties - Part 3: Polyolefin Pipes. International Organization for Standardization, Geneva, Switzerland.

ISO 868-2003, 2003. Plastics and Ebonite - Determination of Indentation Hardness by Means of a Durometer (Shore Hardness). International Organization for Standardization, Geneva, Switzerland.

Khademi-Zahedi, R., 2019. Application of the finite element method for evaluating the stress distribution in buried damaged polyethylene gas pipes. Undergr. Space 4 (1), 59–71. https://doi.org/10.1016/j.undsp.2018.05.002.

Kong, L., Qi, D., Li, H., et al., 2021. Aging of polyethylene of raised temperature resistance pipe liner after a four-Year service in a crude oil gathering system. J. Fail. Anal. Prev. 21 (4), 1323–1330. https://doi.org/10.1007/s11668-021-01176-w.

Li, Y., Liu, W., Ren, X., 2015. Critical stress of high-density polyethylene during stress and photo-oxidative aging. Polym. Eng. Sci. 55 (10), 2277–2284. https://doi.org/10.1002/pen.24114.

Lu, L., Li, X., Gao, J., 2012. Evaluation of aging behavior of medium density polyethylene in natural environment by principal component analysis. J. Appl. Polym. Sci. 125 (1), 19–23. https://doi.org/10.1002/app.34549.

Montes, J.C., Cadoux, D., Creus, J., et al., 2012. Ageing of polyethylene at raised temperature in contact with chlorinated sanitary hot water. Part I–Chemical aspects. Polym. Degrad. Stabil. 97 (2), 149–157. https://doi.org/10.1016/j.polymdegradstab.2011.11.007.

Ojeda, T., Freitas, A., Birck, K., et al., 2011. Degradability of linear polyolefins under natural weathering. Polym. Degrad. Stabil. 96 (4), 703–707. https://doi.org/10.1016/j.polymdegradstab.2010.12.004.

Taherinejad, M., Hosseinalipour, S.M., Madoliat, R., 2017. Dynamic simulation of gas pipeline networks with electrical analogy. J. Braz. Soc. Mech. Sci. 39, 4431–4441. https://doi.org/10.1007/s40430-017-0821-x.

Therias, S., Rapp, G., Masson, C., et al., 2021. Limits of UV-light acceleration on the photooxidation of low-density polyethylene. Polym. Degrad. Stabil. 183 (3), 109443. https://doi.org/10.1016/j.polymdegradstab.2020.109443.

Wang, Q., Zhou, H., Xie, J., et al., 2021. Nonlinear ultrasonic evaluation of high-density polyethylene natural gas pipe thermal butt fusion joint aging behavior. Int. J. Pres. Ves. Pip. 189, 104272. https://doi.org/10.1016/j.ijpvp.2020.104272.

Wang, Y., Lin, D., Xiang, M., et al., 2021. Experimental study on aging performance of polyethylene gas pipelines. IOP Conf. Ser. Earth Environ. Sci. 631, 012066. https://iopscience.iop.org/article/10.1088/1755-1315/631/1/012066.

Weon, J.I., 2010. Effects of thermal ageing on mechanical and thermal behaviors of linear low density polyethylene pipe. Polym. Degrad. Stabil. 95 (1), 14–20. https://doi.org/10.1016/j.polymdegradstab.2009.10.016.

Zha, S., Lan, H.Q., Lin, N., et al., 2023. Degradation and characterization methods for polyethylene gas pipes after natural and accelerated aging. Polym. Degrad. Stabil. 208, 110247. https://doi.org/10.1016/j.polymdegradstab.2022.110247.